MNE 19 (2023) 100195

Contents lists available at ScienceDirect

Micro and Nano Engineering

journal homepage: www.sciencedirect.com/journal/micro-and-nano-engineering

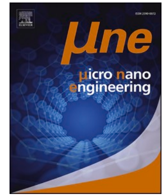

Self-patterned ultra-sharp diamond tips and their application for advanced nanoelectronics device characterization by electrical SPM

L. Wouters *, T. Boehme, L. Mana, T. Hantschel

Imec, Kapeldreef 75, B-3001 Leuven, Belgium

ARTICLE INFO

Keywords:
Diamond tip
Self-patterning
Dry etching
Electrical SPM

ABSTRACT

The continuous downscaling of nanoelectronics devices requires metrology solutions with sub-nanometer spatial resolution. Electrical scanning probe microscopy (E-SPM) techniques such as scanning spreading resistance microscopy have become important tools to map the electronic properties of these devices at nanometer scale using conductive diamond tips. Yet, the spatial resolution that can be achieved in an E-SPM measurement critically depends on the sharpness of the tip being used. Although much progress has already been made in optimizing the tip sharpness, cost-efficiently fabricated high-aspect-ratio diamond tips with ultra-high sharpness are still missing. Therefore, we have developed in this work a dry etching process for super sharp high-aspect-ratio conductive diamond tips, called hedgehog full diamond tips (HFDT), starting from standard low-aspect-ratio full diamond tips (FDT). The distinctive feature of our approach is the self-patterning etch step which benefits the high-volume production of such tips. The self-patterned mask is formed by nanoparticles originating from the interfacial layer deposited during the initial stage of the diamond growth, and metal particles from the surrounding metal cantilever material. In this work, we present our newly developed HFDTs and provide evidence that these tips outperform other conducting tips in terms of spatial resolution during E-SPM measurements.

1. Introduction

Recent innovations in the semiconductor industry with 3D nanometer-sized device architectures such as fin field effect transistors (FinFETs), tunnel-FETs (TFETs), and nanosheet FETs, combined with the implementation of novel materials such as high-k dielectrics, high-mobility channels, and 2D materials, has led to the downscaling of device dimensions towards the range of a few nanometers. Considering the crucial role of metrology in the development and manufacturing control of these devices, also metrology techniques should evolve towards sub-nanometer spatial resolution [1,2]. Electrical scanning probe microscopy (E-SPM) is a technique that offers the possibility to map the electronic properties of devices at the nanometer scale [3]. A sharp micromachined tip is scanned over the surface of a certain sample or device while the current or other electrical properties are being recorded. Scanning spreading resistance microscopy (SSRM) is a well-established E-SPM technique for obtaining quantitative two- and three-dimensional carrier profiles in semiconductor devices [4–7]. In SSRM, it is crucial that a very high pressure of typically 8–12 GPa is formed underneath the tip to ensure an ohmic contact between the tip and the semiconductor sample. The tip needs to be extremely hard to withstand these pressures, highly conductive to minimize parasitic tip resistance and very sharp to obtain high-resolution measurements. These three requirements have made highly boron-doped diamond the material of choice for the fabrication of the tips [8,9].

Two main approaches have been developed for the fabrication of diamond SPM tips: coated diamond tips (CDTs) and full diamond tips (FDTs). A CDT is constructed by depositing a thin (typically 100–300 nm) boron-doped diamond layer on top of a Si tip [10]. The presence of the coating layer increases the initial Si tip radius and therefore limits the tip sharpness that can be achieved. Moreover, breakage of the Si core tip near the apex while scanning at typical SSRM forces in the μN range is a common issue. This complication can be resolved by using an FDT which is made by growing a thick (typically ~1 μm) boron-doped diamond layer in an inverted pyramid mold [11–13]. Here, the diamond tip shape and aspect ratio are defined by the KOH anisotropic etching step that is used to create the pyramid mold [14]. Although FDTs allow for high-resolution E-SPM measurements, their low aspect ratio often causes double-tip and material smearing artifacts. Therefore, diamond tips with a higher aspect ratio and increased sharpness have been developed

* Corresponding author.
E-mail address: lennaert.wouters@imec.be (L. Wouters).

https://doi.org/10.1016/j.mne.2023.100195
Received 14 December 2022; Received in revised form 22 April 2023; Accepted 2 May 2023
Available online 8 May 2023
2590-0072/© 2023 The Authors. Published by Elsevier B.V. This is an open access article under the CC BY-NC-ND license (http://creativecommons.org/licenses/by-nc-nd/4.0/).

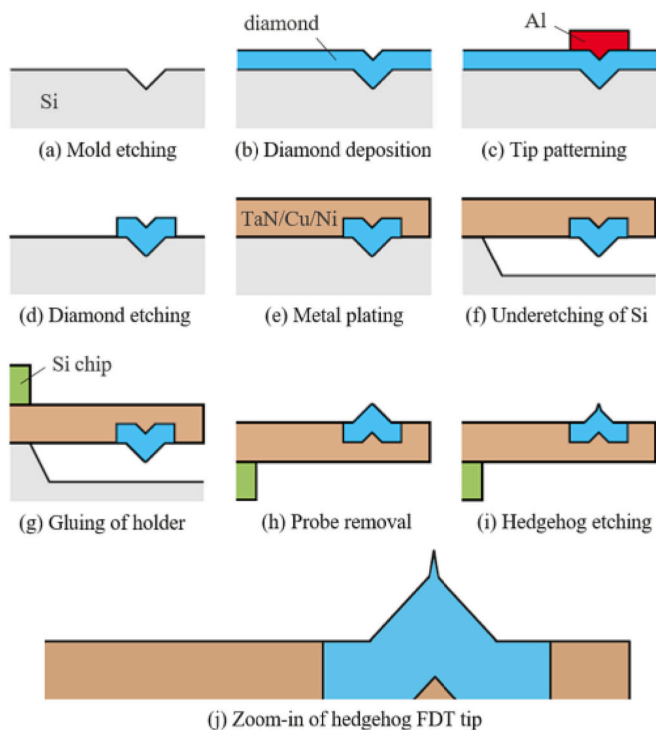

Fig. 1. Schematic representation of the different steps in the HFDT fabrication process.

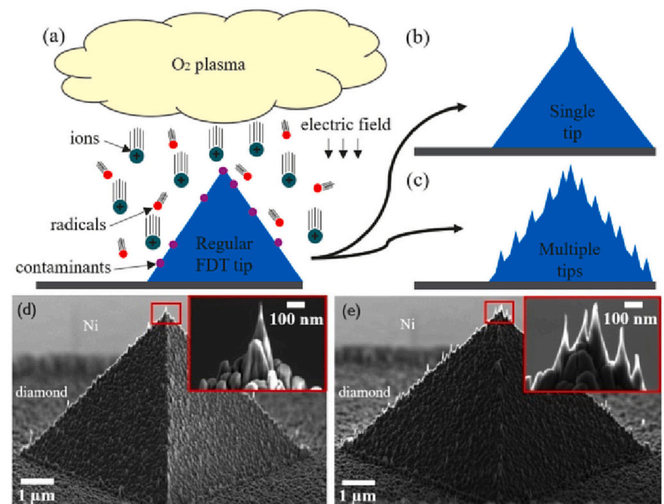

Fig. 2. Schematic representation of the self-patterned O_2 plasma etching process applied to a standard full diamond tip (a) resulting in a hedgehog full diamond tip configuration with a single nanoscopic tip (b) and multiple nanoscopic tips (c) at the pyramid apex. SEM images of single tip (d) and multiple tips (e) configurations.

to overcome these artifacts. An approach with a focused ion beam (FIB) masking step followed by a plasma etching step was used to create a nanoscopic sharp diamond tip on top of a CDT [15]. Furthermore, other diamond tip configurations have been developed, such as single-crystal undoped diamond tips suited for high-resolution morphology measurements [16], and diamond tips with a nitrogen vacancy incorporated at the tip apex for magnetic measurements and quantum sensing applications [17,18].

In this work, we developed the concept for a hedgehog full diamond tip (HFDT) by placing a high-aspect-ratio nanoscopic super sharp tip on top of a conventional low-aspect-ratio pyramid tip. The increased aspect ratio and sharpness of the HFDT configuration overcomes double-tip and smearing artifacts and further improves the resolution of the measurements. Note that our fabrication process is based on self-pattering whereas the aforementioned commercially available nanoscopic sharp tips require a one-to-one FIB treatment of the tip apexes. This paper presents the fabrication process, shows the fabricated tips, and demonstrates their superior performance in E-SPM measurements.

2. Fabrication process

The HFDT fabrication process is identical to the fabrication of the regular FDT probe, as described in detail elsewhere [11], with the addition of one crucial step. A simple representation of the overall process is given in Fig. 1.

First, 7 × 7 μm squares are patterned in a hard mask layer on a Si wafer, followed by anisotropic KOH etching, creating inverted pyramid molds into the silicon (Fig. 1a). The wafer is then seeded with diamond nanoparticles and a highly boron-doped diamond film with a thickness of about 1 μm is grown onto the wafer and in the molds by hot-filament chemical vapor deposition (HF-CVD) (Fig. 1b). In this step, the diamond tip is formed and its shape and aspect ratio are defined. Next, an aluminium layer is sputtered and patterned (Fig. 1c), which acts as the mask to etch the excess diamond by an O_2/SF_6 reactive ion etching (RIE) process (Fig. 1d). A tantalum nitride adhesion/peel-off layer and copper seed layer are sputtered and patterned, followed by the deposition of a 5 μm thick electroplated nickel layer to form the cantilever and membrane (Fig. 1e). The diamond tip and metal cantilever are underetched with KOH (Fig. 1f) after which the probe membrane is peeled away, a metal-coated Si holder chip is glued on the membrane (Fig. 1g) and the probe is removed from the wafer (Fig. 1h) [19].

In this work, we have developed a dry etching process to further convert the standard FDT probe into a super sharp HFDT probe, which is performed in an Oxford Plasmalab 100 etching tool operated at 20 °C, 9 mTorr, 25 W radio-frequency (RF) power and 1200 W inductively coupled plasma (ICP) power. The first step is a 20 s O_2/SF_6 plasma etch with a gas flow rate of 50 sccm for O_2 and 2.5 sccm for SF_6. Fluorine radicals are generated and react with silicon-containing material to remove most of the SiO_xC_y, formed during the initial stages of the diamond growth, from the tip surface [20]. The key step in the process is a 4 min O_2 plasma etching step (Fig. 1i) with an O_2 gas flow rate of 50 sccm. This etching step converts a classical pyramid-shaped FDT into a diamond pyramid with sharp nanoscopic tip(s) on top (Fig. 1j).

3. Fabrication results

Fig. 2a illustrates the O_2 plasma etching step in more detail and depicts the self-patterning feature of the process. Oxygen ions and radicals react with the carbon atoms in the regular diamond tip and etch the diamond away. The surface of the diamond pyramid contains contaminants such as remaining SiO_xC_y residues, nanoparticles from the diamond seeding process [21], and other particles from surrounding materials, e.g. metal particles from the cantilever. These particles have a lower etch rate than diamond and thus can act as a local mask during the etching process. The resulting HFDTs come in two different tip configurations, one configuration with a single sharp tip at the apex of the pyramid base (Fig. 2b) and a second configuration with multiple tips on the pyramid apex (Fig. 2c). Exemplary scanning electron microscopy (SEM) images of both tip configurations are shown in Fig. 2d and Fig. 2e, respectively. The high-resolution images of the tip apexes clearly demonstrate the significantly improved sharpness of the HFDT probes. Tip radiuses down to 2.5 nm have been measured.

Our statistical analysis of the SEM inspections of 63 HFDT probes for the best processes has shown a yield of 39% for sharp single-tip apexes, thus >1/3 of the fabricated tips have a superior aspect ratio and sharpness. These tips are ideal for high-resolution electrical SPM measurements. Additionally, we observed yields of 46% for multiple tips and

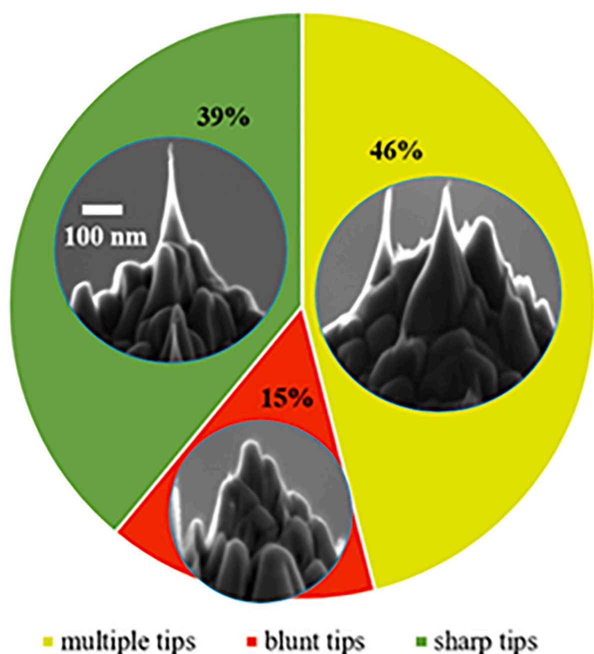

Fig. 3. Pie chart showing the yield of the different tip configurations after plasma etching calculated from the statistical analysis of SEM inspections of 63 HFDT probes.

15% for blunt tips at the pyramid apex (Fig. 3). Note that E-SPM measurements with multi-tip HFDTs initially often still result in high-resolution images, but after a few scans the longest tip wears out and multiple tips start to contact the sample at the same time. This leads to double- or multiple-tip artifacts in the measurement results. These artifacts are not an issue in experiments where material removal is the main focus and therefore multi-tip HFDTs can be used for nano-milling applications. However, we will focus here on the performance of the sharp single-tip HFDTs when evaluating the probes.

To better understand the dynamics of the tip formation, a diamond tip was inspected by SEM at different stages during the HFDT plasma etching. For this study, the etch process was interrupted at certain time intervals; the diamond tip was then inspected with SEM, and afterwards the etching was continued. The SEM image in Fig. 4a shows the presence of two unknown particles on the initial tip structure. Images in Fig. 4b-c are taken during the SF_6 etching step. The SiO_xC_y is removed from the tip and the grainy diamond structure is exposed, while the particles remain unaffected by the SF_6 etching. During the initial stages of the O_2 etching, the diamond is gradually etched away (Fig. 4d-e) and the unknown particles act as an etching mask for tip formation (Fig. 4f-g). The masking particles are etched at a slower rate compared to the diamond but are still getting smaller while the tips grow and get sharper over longer etching times (Fig. 4h), until at some point the masking particles are fully etched and removed (Fig. 4i-j). This is obviously the optimal etching time as can be seen from the SEM image taken at this point with a very sharp tip on top of the base diamond structure. In case of further etching after the particle removal, the tip is overetched and gets a blunt shape. SEM inspection of the HFDT etching of other tips revealed that sometimes new re-sputtered particles end up on the tip during the etching process and start serving as masking particles for the diamond etching. Both cases illustrate the unique self-patterning feature of the developed process and the corresponding tip formation dynamics.

Finally, the composition and origin of the masking particles are investigated by inspecting a remaining particle at the tip apex after the etching process with energy-dispersive X-ray (EDX) analysis (Fig. 5). The spectrum of elements (Fig. 5c) over the yellow box inside the EDX map (Fig. 5b) covering the bulk of the masking particle indicates the abundant presence of Ni atoms. Based on the fabrication process of the diamond tips, it is evident that these particles are originating from the Ni cantilever. This result completes the story explaining the HFDT tip formation during O_2 plasma etching. At the very beginning of the etching, we have nanoscopic masking due to the remaining particles of the early stages of the diamond growth process. However, after the rapid consumption of these initial masking particles, a more stable etch mask is formed mainly by nickel nanoparticles re-sputtered from the surrounding cantilever material.

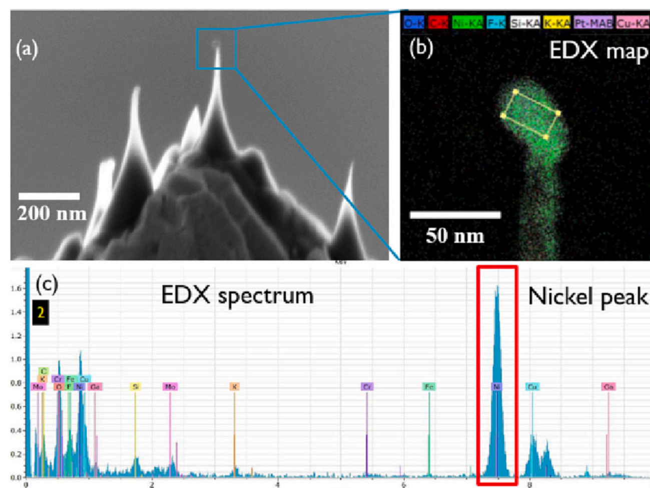

Fig. 5. SEM image (a) and EDX map (b) of a remaining particle at the tip apex after the etching process. EDX spectrum over the yellow box in the EDX map (c). (For interpretation of the references to colour in this figure legend, the reader is referred to the web version of this article.)

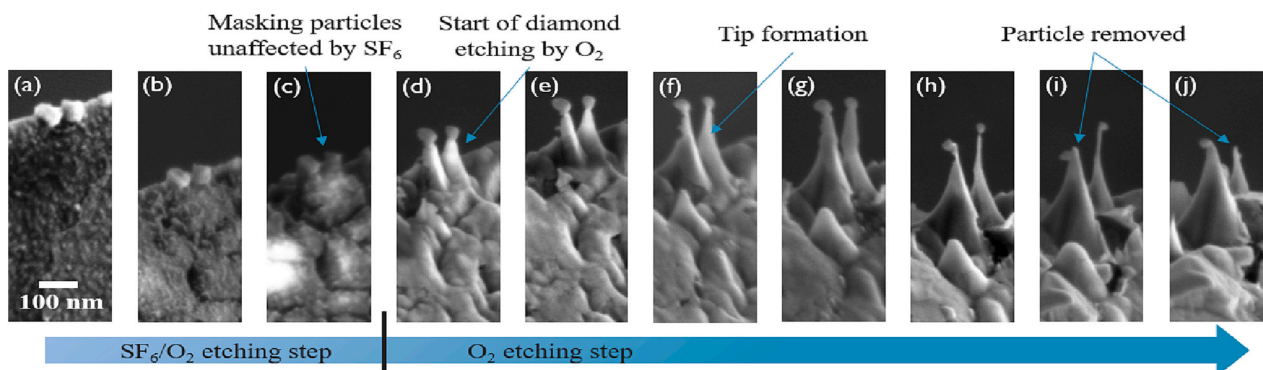

Fig. 4. SEM images taken at different stages during the HFDT etching process.

Table 1
Comparison of different diamond SPM tips.

Name	Reference	Tip fabrication method	Tip radius	Application
Coated diamond tip (CDT)	[10]	Silicon tip etching + diamond CVD	~ 20 nm	Electrical SPM
Full diamond tip (FDT)	[11–13]	Anisotropic etching + diamond CVD + mold removal	5–30 nm	Electrical SPM
Plasma-etched tip on CDT	[15]	CDT + FIB patterning + plasma etching	< 5 nm	Electrical SPM
Single-crystal diamond tip	[16]	Diamond CVD + plasma etching + tip transfer	< 20 nm	Topography AFM
Nitrogen-vacancy diamond tip	[17]	Diamond CVD + electron beam lithography + plasma etching	~ 100 nm	Quantum sensing SPM
Hedgehog full diamond tip (HFDT)	This work	FDT + self-patterning + plasma etching	< 5 nm	Electrical SPM

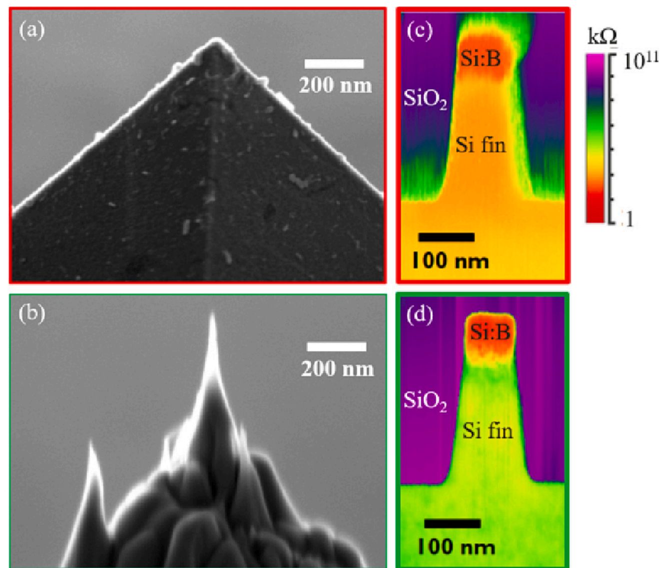

Fig. 6. SEM images of a regular FDT (a) and a super sharp single-tip HFDT (b) tip apex. SSRM resistance map of a 60 nm wide boron-implanted Si fin structure embedded in SiO_2 with a regular FDT (c) and an HFDT (d).

4. Probe evaluation

SEM images have clearly demonstrated the ultra-high sharpness and aspect ratio of the newly developed HFDT probes. A comparison with diamond tips that are already commercially available is shown in Table 1. The tip fabrication method, tip sharpness and applications are listed. As can be seen from the table, certain fabrication methods favor certain applications and vice versa. A more detailed summary on the development of the particular class of E-SPM tips can be found in reference [3]. In this section, the HFDT probes will be tested for their actual use in E-SPM measurements. The E-SPM measurements were performed using a Bruker Dimension Icon-PT AFM system, in a glovebox with Ar environment. SSRM requires highly conductive, wear-resistant, and super-sharp tips and therefore it is an ideal technique for the evaluation of the HFDT probes.

In the first instance, a 60 nm wide boron-implanted silicon fin structure embedded in SiO_2 was investigated with both a conventional FDT and a super sharp single-tip HFDT. SEM images of the apex of the utilized tips and the acquired SSRM 2D resistance maps are shown in Fig. 6. The Si/SiO_2 interface and the boron implant at the top of the fin are much sharper in the SSRM measurement with the HFDT probe as the double-tip artifact in the measurement with the regular FDT tip is overcome. This example provides evidence that our newly developed super sharp conductive diamond tips outperform conventional diamond tips when it comes to spatial resolution. Additionally, the tip showed to be stable over multiple measurements proving that it is sufficiently wear-resistant to be used for semiconductor device metrology.

Fig. 7a and b show correlative 2D SSRM resistance maps and transmission electron microscopy (TEM) images of the cross-section of a 40 nm wide boron-implanted silicon fin structure [22]. The strong resemblance between the two images confirms the high spatial resolution of the SSRM measurement with the HFDT probe. Note that even the nanometer-sized amorphous regions in the top corners of the fin that only get recrystallized after a high-temperature laser anneal can be distinguished in the SSRM resistance map (see Fig. 7c-d).

Additionally, the HFDT probe has proven its value in conductive atomic force microscopy (C-AFM) measurements. C-AFM is a common technique to study the electrical properties of a wide range of materials [14]. In this study, C-AFM is used to study the grain growth in 3D NAND

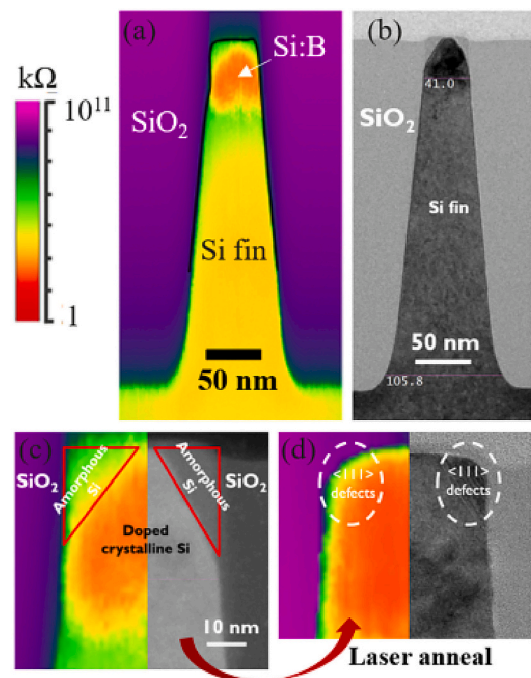

Fig. 7. 2D SSRM resistance map (a) and TEM image (b) of the cross-section of a 40 nm wide boron-implanted Si fin structure embedded in SiO_2; side-by-side comparison of SSRM and TEM images of the boron-implanted region in the fin structure before (c) and after (d) laser annealing.

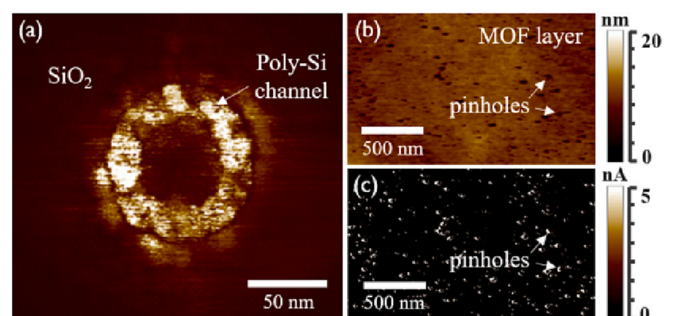

Fig. 8. C-AFM current map of the cross-section of a 3D NAND Si channel after metal-induced lateral crystallization (a); Topography (b) and current map (c) of a metal-organic framework layer.

amorphous Si channels after a metal-induced lateral crystallization (MILC) process [23] and to look for pinholes in metal-organic framework (MOF) layers deposited by chemical vapor deposition [24]. Fig. 8a shows that grainy structures with dimensions in the range of a few nanometers can be identified in the C-AFM current map obtained with an HFDT probe, unlike in measurements obtained with regular FDTs. Similarly, nanoscopic pinholes are observed in both the topography map (Fig. 8a) and the current map (Fig. 8b) of a MOF layer obtained with an HFDT probe, while lots of these pinholes remained invisible in C-AFM measurements with FDTs or commercial metal-coated tips.

5. Conclusions

Our work introduces a process to convert a regular low- aspect-ratio FDT into a super sharp highly conductive and wear-resistant hedgehog FDT probe. The fabrication is based on a self-patterning dry etch process which is a unique process feature compared to other commercial diamond tips and crucial to enable low-cost fabrication. The HFDT probes outperform conventional conductive probes when it comes to spatial resolution in E-SPM measurements. Future work will focus on controlling the masking in order to increase the yield of single sharp tips (currently limited to about one out of three) without adding complexity to the fabrication process.

Declaration of Competing Interest

The authors declare that they have no known competing financial interests or personal relationships that could have appeared to influence the work reported in this paper.

Data availability

Data will be made available on request.

Acknowledgments

We acknowledge Olivier Richard and Pieter Lagrain for TEM inspection and Janusz Bogdanowicz, Steven Folkersma, John Alexander Cruz and Siva Ramesh for providing us with suitable samples for probe evaluation.

References

[1] W. Vandervorst, et al., Dopant, composition and carrier profiling for 3D structures, in: Materials Science in Semiconductor Processing vol. 62, Elsevier Ltd, May 01, 2017, pp. 31–48, https://doi.org/10.1016/j.mssp.2016.10.029.
[2] N.G. Orji, et al., Metrology for the next generation of semiconductor devices, in: Nature Electronics vol. 1, no. 10, Nature Publishing Group, Oct. 01, 2018, pp. 532–547, https://doi.org/10.1038/s41928-018-0150-9.
[3] U. Celano (Ed.), Electrical Atomic Force Microscopy for Nanoelectronics, Springer, Cham, 2019, https://doi.org/10.1007/978-3-030-15612-1.
[4] P. De Wolf, et al., Lateral and vertical dopant profiling in semiconductors by atomic force microscopy using conducting tips, J. Vac. Sci. Technol. A 13 (3) (May 1995) 1699–1704, https://doi.org/10.1116/1.579754.
[5] P. De Wolf, J. Snauwaert, T. Clarysse, W. Vandervorst, L. Hellemans, Characterization of a point-contact on silicon using force microscopy-supported resistance measurements, Appl. Phys. Lett. (1995) 1530, https://doi.org/10.1063/1.113636.
[6] P. De Wolf, T. Clarysse, W. Vandervorst, L. Hellemans, Ph. Niedermann, W. Hänni, Cross-sectional nano-spreading resistance profiling, J. Vac. Sci. Technol. B: Microelectron. Nanometer Struct. 16 (1) (Jan. 1998) 355, https://doi.org/10.1116/1.589810.
[7] P. Eyben, et al., 3D-carrier profiling and parasitic resistance analysis in vertically stacked gate-all-around Si nanowire CMOS transistors, IEEE (2019), https://doi.org/10.1109/IEDM19573.2019.8993636.
[8] J. Snauwaert, N. Blanc, P. De Wolf, W. Vandervorst, L. Hellemans, Minimizing the size of force-controlled point contacts on silicon for carrier profiling, J. Vac. Sci. Technol. B: Microelectron. Nanometer Struct. 14 (2) (Mar. 1996) 1513, https://doi.org/10.1116/1.589129.
[9] W. Kulisch, A. Malave, G. Lippold, W. Scholz, C. Mihalcea, E. Oesterschulze, Fabrication of integrated diamond cantilevers with tips for SPM applications, Diam. Relat. Mater. 6 (5–7) (Apr. 1997) 906–911, https://doi.org/10.1016/S0925-9635(96)00600-0.
[10] Ph. Niedermann, W. Hänni, N. Blanc, R. Christoph, J. Burger, Chemical vapor deposition diamond for tips in nanoprobe experiments, J. Vac. Sci. Technol. A 14 (3) (May 1996) 1233–1236, https://doi.org/10.1116/1.580273.
[11] T. Hantschel, et al., Diamond scanning probes with sub-nanometer resolution for advanced nanoelectronics device characterization, Microelectron. Eng. 159 (Jun. 2016) 46–50, https://doi.org/10.1016/j.mee.2016.02.053.
[12] T. Hantschel, P. Niedermann, T. Trenkler, W. Vandervorst, Highly conductive diamond probes for scanning spreading resistance microscopy, Appl. Phys. Lett. 76 (12) (Mar. 2000) 1603–1605, https://doi.org/10.1063/1.126109.
[13] T. Hantschel, et al., Conductive diamond tips with sub-nanometer electrical resolution for characterization of nanoelectronics device structures, Phys. Status Solidi A 206 (9) (Sep. 2009) 2077–2081, https://doi.org/10.1002/pssa.200982212.
[14] H. Seidel, L. Csepregi, A. Heuberger, H. Baumgärtel, Anisotropic etching of crystalline silicon in alkaline solutions: I. orientation dependence and behavior of passivation layers, J. Electrochem. Soc. 137 (11) (Nov. 1990) 3612–3626, https://doi.org/10.1149/1.2086277.
[15] S.K. Tripathi, et al., Resolution, masking capability and throughput for direct-write, ion implant mask patterning of diamond surfaces using ion beam lithography, J. Micromech. Microeng. 22 (5) (May 2012), https://doi.org/10.1088/0960-1317/22/5/055005.
[16] A.N. Obraztsov, P.G. Kopylov, B.A. Loginov, M.A. Dolganov, R.R. Ismagilov, N. V. Savenko, Single crystal diamond tips for scanning probe microscopy, Rev. Sci. Instrum. 81 (1) (2010), https://doi.org/10.1063/1.3280182.
[17] P. Maletinsky, et al., A robust scanning diamond sensor for nanoscale imaging with single nitrogen-vacancy centres, Nat. Nanotechnol. 7 (5) (2012) 320–324, https://doi.org/10.1038/nnano.2012.50.
[18] A. Schmidt, T. Jaffe, M. Orenstein, J.P. Reithmaier, C. Popov, Fabrication of diamond AFM tips for quantum sensing, in: P. Petkov, M.E. Achour, C. Popov (Eds.), Nanoscience and Nanotechnology in Security and Protection against CBRN Threats, Springer Netherlands, Dordrecht, 2020, pp. 171–185, https://doi.org/10.1007/978-94-024-2018-0_13.
[19] T. Hantschel, S. Slesazeck, N. Duhayon, M. Xu, W. Vandervorst, Peel-off probe: A cost-effective probe for electrical atomic force microscopy, in: Materials and Device Characterization in Micromachining III, SPIE, Aug. 2000, p. 50, https://doi.org/10.1117/12.395612.
[20] M. Tsigkourakos, et al., Suppression of boron incorporation at the early growth phases of boron-doped diamond thin films, Phys. Status Solidi A 212 (11) (Nov. 2015) 2595–2599, https://doi.org/10.1002/pssa.201532185.
[21] M. Tsigkourakos, T. Hantschel, K. Arstila, W. Vandervorst, Diamond nano-particle seeding for tip moulding application, Diam. Relat. Mater. 35 (May 2013) 14–18, https://doi.org/10.1016/j.diamond.2013.03.008.
[22] S. Folkersma, et al., Apparent size effects on dopant activation in nanometer-wide Si fins, J. Vac. Sci. Technol. B 39 (2) (Mar. 2021), 023202, https://doi.org/10.1116/6.0000921.
[23] S. Ramesh, et al., Understanding the kinetics of metal induced lateral crystallization process to enhance the poly-Si channel quality and current conduction in 3-D NAND memory, in: 2021 IEEE International Electron Devices Meeting (IEDM), IEEE, Dec. 2021, https://doi.org/10.1109/IEDM19574.2021.9720571, 10.2.1-10.2.4.
[24] A.J. Cruz, et al., Integrated cleanroom process for the vapor-phase deposition of large-area Zeolitic Imidazolate framework thin films, Chem. Mater. 31 (22) (Nov. 2019) 9462–9471, https://doi.org/10.1021/acs.chemmater.9b03435.